

# ADM-MODELLING APPROACH FOR SEMI-DIRECT NUMERICAL SIMULATION OF TURBULENT MIXING AND MASS TRANSPORT

**Florian Schwertfirm, Michael Manhart**

Fachgebiet Hydromechanik,  
TU München  
Arcisstrasse 21, 80333 München  
f.schwertfirm@bv.tum.de

## ABSTRACT

This paper presents a model for calculating turbulent mixing and mass transport in high Schmidt number flows based on a Direct Numerical Simulation of the flow field and a solution of the filtered transport equation of the scalar field. We call this approach SEMI-DNS. It is shown that, in this strategy, the only term that needs to be modelled is the cross stress term  $C_i = \overline{u_i c'}$ , which eases modelling of the unresolved scales of the scalar field considerably. An a-priori analysis of the DNS data of turbulent channel flow at  $Re_\tau = 180$  and  $Sc = 3$  and  $Sc = 10$  shows that this term is small. Because of the quasi linearity of the scalar transport equation, the ADM model is applied for this term, and SEMI-DNS calculations are performed up to  $Sc = 1000$ . Comparisons with full DNS results up to  $Sc = 10$  and global quantities from the literature up to  $Sc = 1000$  show excellent agreement.

## INTRODUCTION

In recent years, Direct Numerical Simulation (DNS) of low Reynolds number flows became readily available to the CFD community, providing reference data and insight for turbulent flow problems. A counter example is turbulent mixing at high Schmidt numbers. In that case, where the diffusion of the scalar quantity is much smaller than the molecular momentum exchange, the length scales of the scalar field are, due to permanent folding and straining motion of the smallest eddies, much shorter than the smallest length scales in the fluid. Batchelor (1959) derived a scaling law for the length scale as:

$$\eta_B = \frac{\eta_K}{\sqrt{Sc}} \quad , \quad (1)$$

where  $\eta_K$  is the Kolmogorov scale and  $Sc$  the Schmidt number. For realistic fluids  $Sc$  can take a wide range of values, from  $Sc = 1$  for pollutant in air to  $Sc = 2000$  for a tracer in water. In the case for very high  $Sc$  Direct-Numerical-Simulation (DNS) becomes cumbersome if not impossible, as the required grid resolution scales with  $Sc^{3/2}$ .

The standard solution for this is to perform a Large-Eddy Simulation (LES) for the mixing process, in which not all relevant length scales are resolved. When a spatial filter operation is applied on the scalar transport equation, we obtain the time evolution of the filtered concentration field  $\bar{c}$  as

$$\frac{\partial \bar{c}}{\partial t} + \frac{\partial \overline{u_j c}}{\partial x_j} = \frac{\nu}{Sc} \frac{\partial^2 \bar{c}}{\partial x_j^2} \quad . \quad (2)$$

Here  $c$  is the concentration of species,  $u_i$  the velocities in cartesian coordinates and  $\nu$  the kinematic viscosity. Here we

are confronted with the convective term leading to an unclosed equation as the term  $\overline{u_j c}$  can not be computed exactly with the available filtered quantities  $\overline{u_j}$  and  $\bar{c}$ . So equation (2) is written as

$$\frac{\partial \bar{c}}{\partial t} + \frac{\partial \overline{u_j c}}{\partial x_j} = \frac{\nu}{Sc} \frac{\partial^2 \bar{c}}{\partial x_j^2} - \frac{\partial}{\partial x_j} M_i \quad . \quad (3)$$

The sub grid scale mass flux  $M_i^\alpha$  is defined as

$$M_i = \overline{u_i c} - \overline{u_i} \bar{c} \quad . \quad (4)$$

The standard approach is to relate the sub grid scale mass fluxes to the mean scalar gradient in analogy to the eddy viscosity models, which implies that the turbulent mass flux is aligned with the filtered scalar gradient and that it is related directly to the eddy viscosity. Additional mixing is produced by, in the terms of the filter width, non-resolved eddies. Consequently the microscale mixing taking place at scales smaller than the Kolmogorov scale is not taken into account at all. If the flow field is calculated by DNS and only the scalar field is under resolved as a high  $Sc$ -number is regarded, this approach fails. First the turbulent viscosity is not available. Second, there are no non-resolved eddies which could account for additional mixing.

In this paper, we present a model for the calculation of scalar fields for high  $Sc$  numbers in combination with DNS of the flow field, thus enabling to produce accurate results for a wide range of  $Sc$ . Because of the combination of DNS for the flow field and modelling of the scalar transport equation, we speak of a SEMI-Direct Numerical Simulation (SEMI-DNS). We first present the basic definitions for SEMI-DNS, propose a model for the unclosed scalar transport equation and undertake a-priori analysis of DNS data for turbulent mixing in channel flow at  $Re_\tau = 180$  and up to  $Sc = 10$ . Finally we apply the developed ideas to a SEMI-DNS of the turbulent channel flow up to  $Sc = 1000$  and compare the results with DNS data and global quantities from the literature.

## SEMI DIRECT APPROACH

When increasing the  $Sc$  number, the Batchelor scale gets much smaller than the Kolmogorov scale (equation 1), leading to sheet like structures within the smallest eddies. By resolving the flow field till the Kolmogorov scale, and applying a filter with a filter width of the same order as  $\eta_K$  we can assume that the quantities of the flow field, namely the velocities  $u_i$  and the pressure  $p$  are not altered by the filter operation:

$$u_i(x) \approx G * u_i(x) = \int G(x - x'; \Delta) u_i(x') dx' \quad (5)$$

$$p(x) \approx G * p(x) = \int G(x - x'; \Delta) p(x') dx' \quad (6)$$

In this case, when  $\Delta \approx \eta_K$ , we note that  $u_i = \bar{u}_i$  and  $u'_i = 0$ . According to Leonard (1974) we decompose the convective term in equation (4) in filtered and sub-filtered part and by applying the definition (5) only the following terms remain

$$M_i = \overline{u_i \bar{c}} - u_i \bar{c} + \overline{u_i c'} \quad (7)$$

We call  $L_i = \overline{u_i \bar{c}} - u_i \bar{c}$  the Leonard term and  $C_i = \overline{u_i c'}$  the cross stress term<sup>1</sup>. Inserting this into equation (3) we get

$$\frac{\partial \bar{c}_\alpha}{\partial t} + \frac{\partial \overline{u_j \bar{c}_\alpha}}{\partial x_j} = \frac{\nu}{Sc} \frac{\partial^2 \bar{c}_\alpha}{\partial x_j^2} - \frac{\partial \overline{u_j c'_\alpha}}{\partial x_j} \quad (8)$$

In this equation the cross stress term has to be modelled. It is revealing to look at the triad interaction in Fourier space of the term  $u_i c$ :

$$u_i(\vec{x}, t) c_\alpha(\vec{x}, t) = \sum_{\vec{k}', \vec{k}''} \delta_{\vec{k}, \vec{k}' + \vec{k}''} e^{i\vec{k}\vec{x}} \hat{u}_i(\vec{k}', t) \hat{c}(\vec{k}'', t) \quad (9)$$

where  $\vec{k}$  is the wavenumber vector and  $\hat{u}_i(\vec{k}, t)$  and  $\hat{c}(\vec{k}, t)$  are the Fourier coefficients of the specific wavenumber. Speaking of our SEMI-DNS, we are only interested in the time evolution of the filtered concentration field and therefore only in an interaction of the convective term which produces wavenumber smaller than  $|\vec{k}_\eta| = 2\pi/\eta_K$ . As the wavenumber for the velocity  $\vec{k}'$  are by definition (5) always smaller than  $|\vec{k}_\eta|$ , the only unknown term in equation (7) which contributes to the wavenumber range in question is the cross stress  $C_i$  with  $|\vec{k}_\eta| < |\vec{k}''| < 2|\vec{k}_\eta|$ . Wavenumbers of the scalar-spectrum larger than  $2|\vec{k}_\eta|$  have no contribution to the time evolution of scalar modes with  $|\vec{k}''| < |\vec{k}_\eta|$ , independent of  $Sc$ . The modelling is therefore reduced to the scales between  $\eta_K$  and  $\eta_K/2$ , as we compute a DNS of the flow field and an LES of the scalar field. The cross stress  $C_i$  which influences the time evolution of the filtered concentration field is confined to a small band of physical scales, therefore we expect it to be small. For a constant velocity within the filter width the cross stress would even be equal to zero, as the velocity could be moved out from the filter operation. As this is a quasi-linear problem we apply the Approximate Deconvolution Model (ADM) as proposed by Stolz and Adams (1999) and modified by Mathew et al. (2003) for modelling  $M_i$ , as it is basically a plain filter operation.

## MODELLING

As in a classical LES, the ADM approach we apply here is based on filtering the quantities with a spatial filter:

$$\bar{c}(x) = \int G(x - x'; \Delta) c(x') dx' \quad (10)$$

The sub grid scale mass flux is calculated by constructing an approximate  $\tilde{c}$  to the full and unfiltered concentration field  $c$ . So equation (4) can be rewritten as

$$M_i = \overline{u_i \tilde{c}} - u_i \bar{c} \quad (11)$$

<sup>1</sup>this decomposition is the same to the Leonard decomposition of the SGS-term in LES, the quantities here are vectors instead of tensors. The Residual stress term  $R_i = u'_i c' = 0$  and the cross stress  $\overline{u'_i \bar{c}} = 0$  due to the definition of the SEMI-DNS

With the definition of the SEMI-DNS, the velocities need no special treatment, as they are calculated exactly with the used resolution and filter width.  $\tilde{c}$  is constructed by inverting the filter operation (10). Meaningful filters are not invertible, so an approximate deconvolution is defined by truncating the series expansion of the inverse operation  $Q$  at a certain  $N$

$$Q_N = \sum_{\nu=0}^N (I - G)^\nu, \quad (12)$$

where  $I$  is the identity operation. This defines the approximately de-convolved quantity:

$$\tilde{c} = Q_N * G * c \quad (13)$$

which is also a filter operation, with  $c = \tilde{c} + c''$  where  $c''$  is the sub filter fluctuation. Domaradzki and Adams (2002) note that in LES calculations of turbulent flows, the ADM for the sub grid scale tensor  $\tau_{ij}$  would only model the account of  $\tau_{ij}$  which can be expressed on the LES grid. For this reason an additional filter step was introduced which stands for the dissipation to the sub grid-scales which are smaller than the Nyquist-criteria of the grid, the so called regularisation term. However, their LES simulations were reported to be quite insensitive to this parameter (Stolz and Adams 1999, Stolz et al. 2001 and Domaradzki and Adams 2002). This method was reviewed by Mathew et al. (2003). He showed that the effect of deconvolution and regularisation are equal to one single explicit filtering step. When inserting equation (11) with the definition (13) and (5) in equation (3) we obtain

$$\frac{\partial \bar{c}}{\partial t} + \frac{\partial \overline{u_j \bar{c}}}{\partial x_j} = \frac{\nu}{Sc} \frac{\partial^2 \bar{c}}{\partial x_j^2} - \frac{\partial}{\partial x_j} \overline{u_j c''}. \quad (14)$$

Equation (14) can be integrated in time numerically and the filtering and de-filtering step is applied subsequently. Thus, first the quantity  $\bar{c}^{(N)}$  at the time level  $N$  is de-convolved with  $Q_N$  to get  $\tilde{c}^{(N)}$ . With it  $\tilde{c}^{(N+1)}$  at the new time level is calculated by numerical integration, followed by a filtering step with  $G$  to finally get  $\bar{c}^{(N+1)}$ . In this procedure filtering is directly followed by de-filtering in consecutive time steps and thus the single filtering operation with the filter  $Q_N G$  can be applied on the concentration field after each time step. So we can rewrite equation (14) for the time evolution of filtered scalar fields, with the filter  $Q_N * G$ , and the definition (5) as

$$\frac{\partial \tilde{c}}{\partial t} + \frac{\partial \overline{u_j \tilde{c}}}{\partial x_j} = \frac{\nu}{Sc} \frac{\partial^2 \tilde{c}}{\partial x_j^2} - \frac{\partial}{\partial x_j} \overline{u_j c''}. \quad (15)$$

The last term on the right hand side of equation (15) represents the cross term arising from the sub filter fluctuations. This term cannot be represented by deconvolution and is the reason for introducing the regularisation term. As Mathew et al. (2003) showed that the regularisation term is similar to apply an additional explicit filtering every time step, regularisation and ADM can be achieved by applying one filter with a specific transfer function. As a consequence, this means that the ADM model applied to the filtered scalar transport equation consist of removing the high wavenumber content of  $c$  thus setting the cross stress term  $C_i = \overline{u_i c''}$  to zero. Consequently, the performance of the model will be good when this term is small.

## NUMERICAL METHOD

### Flow Solver

For the following computations of the flow field, the code MGLET is used (Manhart and Friedrich 2002, Manhart 2004). The incompressible Navier-Stokes equations, namely the conservation of mass and momentum, are solved in Finite Volume (FV) formulation on a Cartesian grid, using a staggered variable arrangement. The discretisation in space of the transported and transporting quantities at the cell faces is fourth order accurate (Kobayashi, 1999) and for the integration in time a third order Runge-Kutta method is used. The incompressibility constraint is satisfied by solving the Poisson-equation for the pressure with an Incomplete Lower-Upper (ILU) decomposition and applying a correction step for the velocities and the pressure which is second order accurate.

### Discrete Filter

For the scalar field a filter with a specific transfer function  $Q_N G$  is applied successively for each spatial direction. As the computations are carried out for fully developed turbulent channel flow, two different filters are required. One for the periodic directions and one for the non-equidistant wall normal direction. For the wall normal direction, we follow Stolz and Adams (1999) and use a five point stencil to define an explicit filter  $G$  in physical space. By applying equation (12) with  $\nu = 6$  we get the filter  $Q_N G$ , which is shown in figure (1). For the periodic directions a spectral filter is used. The scalar field is transformed into wavenumber space, where each wavenumber is multiplied by the amplification factor which stems from the desired transfer function. The transfer function is constructed according to Lele (1992) to match the shape of the transfer function of the explicit wall-normal filter  $Q_N G$ , and is also depicted in figure(1).

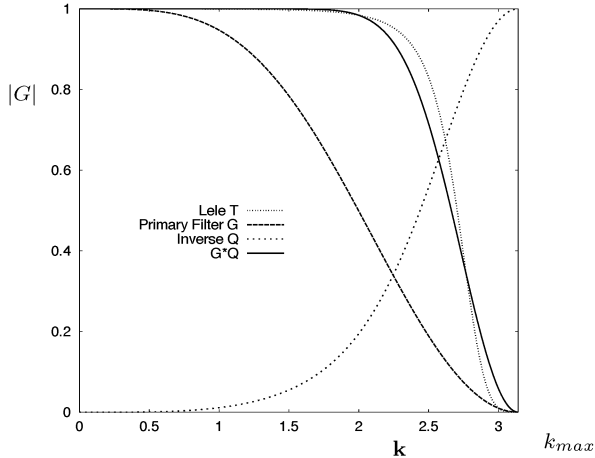


Figure 1: Transfer functions of the explicit primary filter  $G$ , the approximate inverse  $Q_N$ , the resulting filter  $G * Q_N$  and spectral filter (Lele, 1992) applied in homogeneous directions.

## RESULTS

For validation, mass transfer calculations were carried out in a fully developed turbulent channel flow at  $Re_\tau = 180$ , built with the friction velocity  $u_\tau$ , the half channel height  $h$  and the kinematic viscosity  $\nu$ . Three different  $Sc$  numbers of 1, 3 and

Table 1: Information on grid and statistics of the DNS calculations

	grid A	grid B	grid C
resolution	128x80x128	256x160x256	388x240x388
$\Delta x^+$	9.05	4.525	3.013
$\Delta y^+$	7.24	3.62	2.41
$\Delta z^+$	1.35 - 4.98	0.67 - 2.49	0.44 - 1.63
DNS at SC	1	3	10
sample t $\frac{\nu}{u_\tau}$	10380	3690	1470
nr. of samples	1500	800	640

10 were computed by a full DNS. The channel flow is periodic in the stream- and span-wise direction, hereafter referred as  $x$ - and  $y$ -direction. At the walls, there is a no-slip boundary condition for the velocities, whereas the scalar was added at the lower wall and removed at the upper wall by keeping the concentration constant at  $c(x, y, 0) = 1.0$  and  $c(x, y, 2h) = -1.0$ . Compared to other simulations of the turbulent channel flow (Kim et. al. 1987, Kasagi and Iida 1999, Na and Hanratty 2000) the domain size was reduced to  $(2\pi h, \pi h, 2h)$  in order to keep the computational effort feasible for the DNS of the scalar field at  $Sc = 10$ . The resolutions (B) and (C) are scaled with  $\approx \sqrt{Sc}$  compared to grid (A), for further details see table (1) Computations were also carried out with  $Sc = 1.0$  on grid (B) to study the grid dependence. The calculations for the SEMI-DNS at  $Sc = 3, 10, 100$  and  $1000$  were all carried out on grid (A).

All variables are made dimensionless with the friction velocity  $u_\tau = (\tau_w / \rho)^{1/2}$ , the inner coordinate  $z^+ = z \cdot u_\tau / \nu$  as well as the mass flux at the wall  $c_\tau = \nu / (Sc u_\tau) \cdot (\partial c / \partial z)$ .

### Validation of the DNS computations

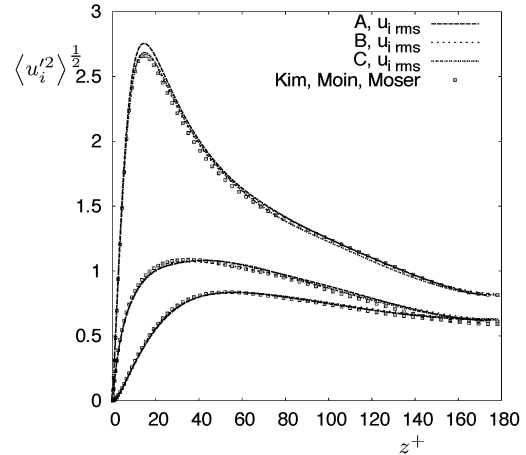


Figure 2: Comparison of velocity  $rms$ -values of the DNS calculations with reference data from Kim et. al. (1987).

Figure (2) shows the  $rms$ -values of the velocity for grid (A), (B) and (C) and the reference data of Kim et al. (1987). The agreement of the data is very good, although there is a slight overshoot of the  $u_{rms}$  values at  $z^+ = 15$  on grid (A). This overshoot reduces as the resolution is increased, and the results of grid (B) and (C) are almost indiscernible and agree very well with the data of Kim et al. (1987).

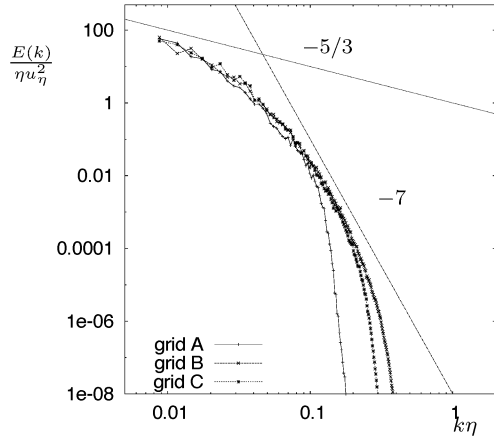


Figure 3: Stream-wise energy spectrum of the u-velocity at  $z^+ = 100$  at different resolutions; normalised by Kolmogorov scales.

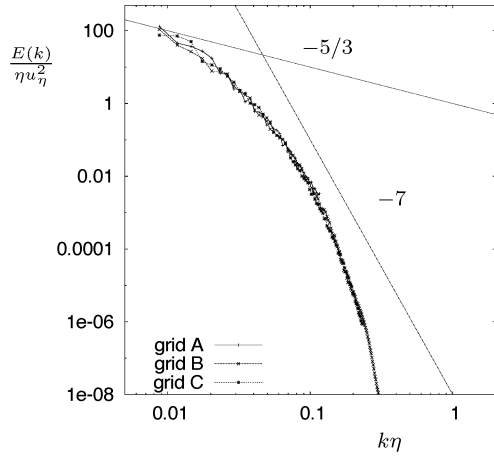


Figure 4: Span-wise energy spectrum of the u-velocity at  $z^+ = 100$  at different resolutions; normalised by Kolmogorov scales.

The span-wise and stream-wise spectra (figure 3 and 4) show almost no inertial range, which is due to the low Reynolds-number. There is a smooth transition to the dissipation range and the spectra lie on top of each other for the different resolutions, which shows the convergence of the solution on grid (A). In the spectra in x-direction we see a damping appearing at approximately  $k_{max}/2$ , which is due to the numerical scheme. However, as the energy decays for four magnitudes before this damping appears and as in this flow configuration the scales responsible for the bulk of dissipation are considerably larger than the Kolmogorov length scale, we regard the resolution of grid (A) still as adequate. To validate our DNS results of the scalar field, we computed the scalar field at  $Sc = 1$  also on grid (B). The *rms* of the concentration on grid (A) and (B) at  $Sc = 1$  show a negligible underestimation of the scalar fluctuation in the channel centre at grid (A). Therefore, we consider the solution of  $Sc = 1$  as converged on grid (A).

#### A-priori analysis of SEMI-Direct Simulation

The results of the DNS-Simulations at  $Sc = 3$  and  $Sc = 10$  were used to analyse a-priori the performance of the model

idea. As mentioned before, the magnitude of the term  $\widetilde{u_i c''}_\alpha$  determines the model performance. In our case, grid (A) is adequate to represent all relevant length scales of the flow field. So we can calculate the term  $\widetilde{u_i c''}$  for  $Sc = 3$  and  $Sc = 10$  on grid (A):

$$C_i = \widetilde{u_i c''} = \widetilde{u_i c} - \widetilde{u_i} \widetilde{c} \quad (16)$$

By setting the cut off wavenumber of the filter  $\widetilde{\Delta}$  to  $k_c = \frac{\pi}{\Delta x_i}$  where  $\Delta x_i$  is the grid spacing in  $x$ - and respectively  $y$ -direction of grid (A), we can calculate all the cross stresses which can not be represented on grid (A). We applied a sharp spectral filter in the homogeneous  $x$ - and  $y$ -direction on one instantaneous flow- and scalar-field of the DNS data of the channel flow at  $Sc = 3$  and  $Sc = 10$  with the cut-off wavenumber  $k_c$ . Although this is in the range of 9 to 10 times the Kolmogorov length scale of the channel flow, it is still acceptable considering the presented spectra. The *rms* value of the cross stress  $C_i$  was normalised with the *rms* of  $\widetilde{u_i c}$ :

$$\epsilon = \frac{\langle \widetilde{u_i c''}^2 \rangle^{1/2}}{\langle \widetilde{u_i c}^2 \rangle^{1/2}} \quad (17)$$

where  $\langle \rangle$  denotes the average over the homogeneous directions and the upper and lower channel half.

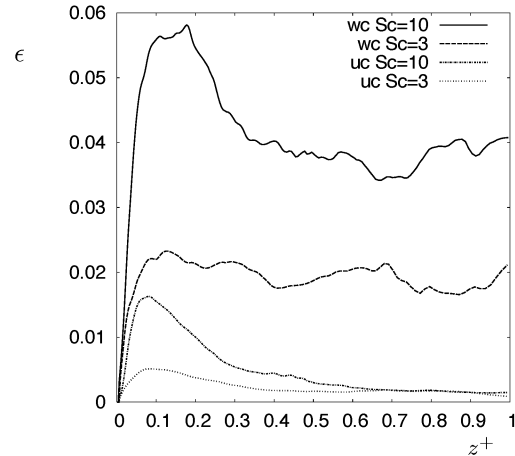


Figure 5: A-priori estimation of the model error  $\epsilon$  on grid (A), from DNS at  $Sc = 3$  grid (B) and DNS  $Sc = 10$  on grid (C).

As figure (5) shows,  $\epsilon$  is at 2% at  $Sc = 3$  and at 4 – 6% at  $Sc = 10$  for  $\widetilde{w c''}$ , as well as lower than 1% at  $Sc = 3$  and between 1.5 and 0.5% at  $Sc = 10$  for  $\widetilde{u c''}$ . It has a peak close to the wall, increasing with increasing  $Sc$ . For  $\widetilde{u c''}$  the cross stress in the centre of the channel doesn't change with  $Sc$ , in the case for  $\widetilde{w c''}$  it is almost doubled. This is due to the reduction of the wall normal mass flux  $\widetilde{w c}$  with increasing  $Sc$ . For the considered  $Sc$  the cross stress term is small, and as such the ADM model is expected to work well.

#### SEMI-DNS SIMULATIONS

In figure (6) the mean concentration profiles  $\langle c \rangle$  of DNS and the SEMI-DNS are compared for different  $Sc$ . The mean concentration profiles show no deviation between DNS and SEMI-DNS calculation. In the viscous sub layer all curves follow the linear law of the wall  $\langle c^+ \rangle = Sc \cdot z^+$ . The concentration fluctuations depicted in figure (7) show also a very

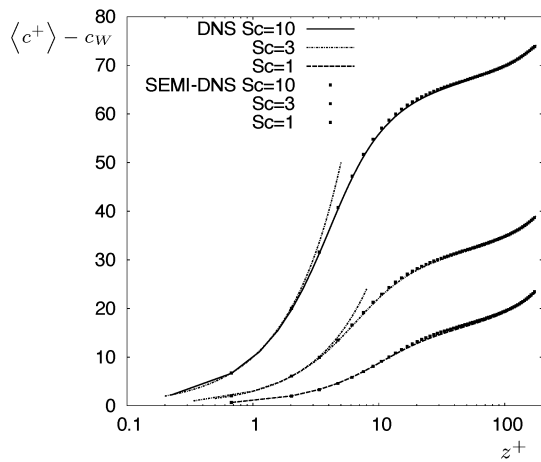


Figure 6: Mean concentration profiles in semi logarithmic coordinates, linear law of the wall  $\langle c^+ \rangle = Scz^+$ .

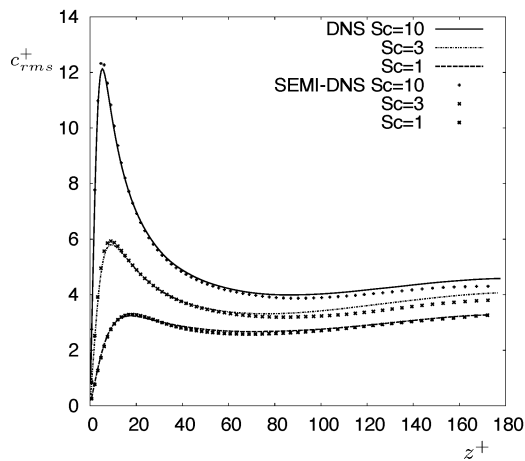


Figure 7: rms of the concentration at different  $Sc$ .

good agreement. The differences in the fluctuations increase with higher  $Sc$  and to the centre of the channel, because there is more fluctuation energy in higher wavenumbers at higher  $Sc$ , so the effect of the filtering has more impact on the fluctuations. At  $Sc = 1$  there is no difference between the DNS and SEMI-DNS simulation, as the the Kolmogorov length scale is equal to the Batchelor length scale, and both are properly resolved on grid (A).

The turbulent mass fluxes  $\langle u'c' \rangle$  and  $\langle w'c' \rangle$  (figure 8 and 9) also show an excellent agreement. In accordance to the a-priori analysis, the error in  $\langle u'c' \rangle$  is smaller than in  $\langle w'c' \rangle$ , although for  $\langle w'c' \rangle$  the statistics for the DNS at  $Sc = 10$  are not yet fully converged. At  $Sc = 10$  the Batchelor scale is approximately 3 times smaller than the Kolmogorov length scale which implies that the scale separation is small. To see if the model is capable to predict very high Schmidt number mixing, calculations with  $Sc = 100$  and  $Sc = 1000$  were done on grid (A). The only way to validate those results was to compare the dimensionless mass transfer coefficients with the values at  $600 < Sc < 39300$  provided by Shaw and Hanratty (1977) for turbulent pipe flow. In figure (10) the results of the SEMI-DNS, the empirical curves by Shaw and Hanratty (1977) and the numerical results of Na et al. (1999) are shown.

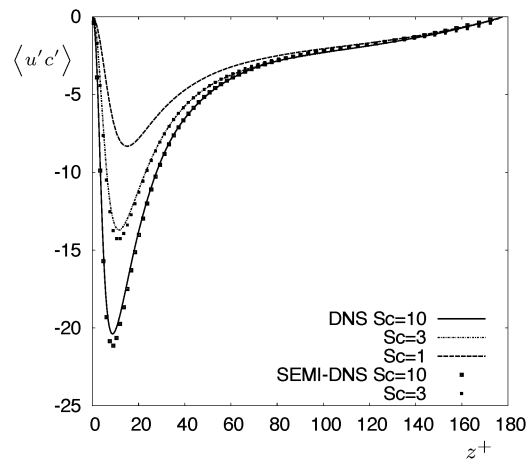


Figure 8: Turbulent mass flux  $\langle u'c' \rangle$  for different  $Sc$ .

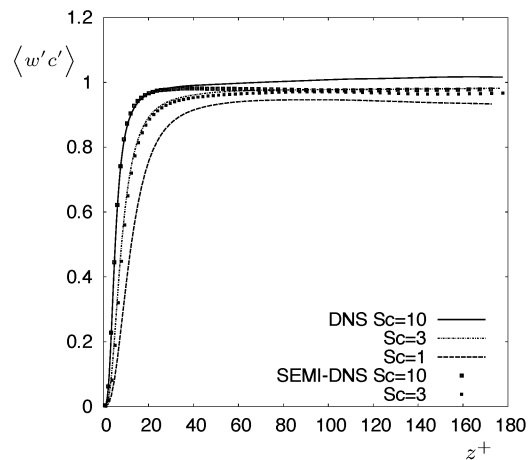


Figure 9: Turbulent mass flux  $\langle w'c' \rangle$  for different  $Sc$ .

The agreement is very good, despite the difference in  $Re_\tau$  to the simulations of Na et al. and despite the measurements of Shaw are for pipe and not for channel flow.

For the simulations at  $Sc = 100$  and  $Sc = 1000$  the mean concentration field and the concentration fluctuations are shown in figures (11) and (12). With increasing  $Sc$ , the gradient at the wall of the mean temperature increases, until almost all the change of the mean temperature field takes place within 10% of the half channel height  $\delta$ . Accordingly, the peaks of the temperature fluctuations move closer to the wall and gets more pronounced. Na and Hanratty (2000) state that the thickness of the diffusive sub layer scales with  $\Delta\theta \propto 1/\sqrt{Sc}$ . This implies that for the high  $Sc$  numbers, the diffusive sub layer, where the highest gradients appear, is not resolved at all, and that for wall bounded problems the need for a special wall model comes up.

## CONCLUSION

A new method for the simulation of turbulent flows with passive scalar transport at high  $Sc$  was developed. This method requires a DNS of the turbulent flow, restricting it on the one hand to low  $Re$  flow, where a DNS is feasible. On the other hand it was shown that by fully resolving the flow field and using the ADM to model the scalar transport, very

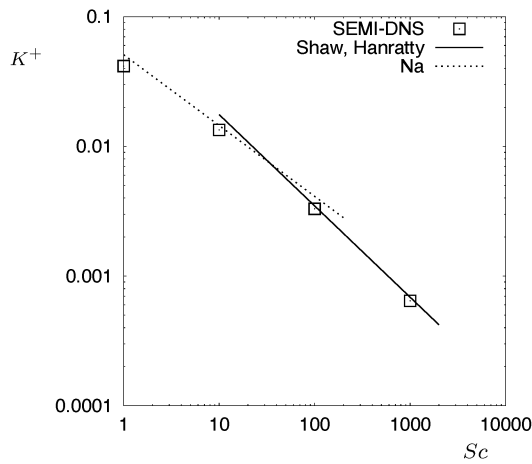


Figure 10: Mass transfer coefficient  $K^+$ ; Shaw and Hanratty(1977):  $0.0889Sc^{-0.704}$ ; Na et. al. (1999):  $0.0509Sc^{-0.546}$

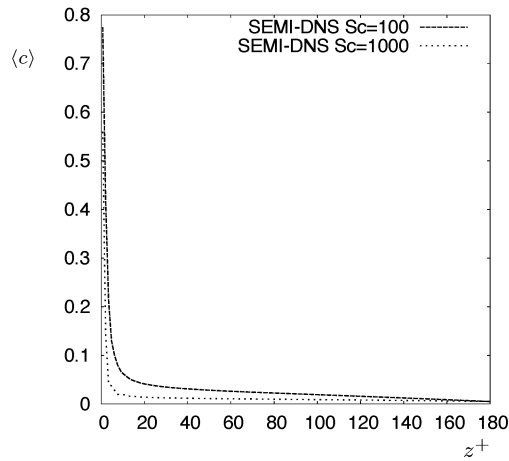


Figure 11: Mean concentration profile (absolut) at  $Sc = 100$  and  $Sc = 1000$

accurate results for the filtered scalar fields can be achieved. Up to  $Sc = 10$  the DNS and SEMI-DNS show almost perfect agreement. Additionally, it was possible to determine the mass transfer coefficient  $K^+$  at  $Sc = 1000$  accurately and to provide results for the mean and  $rms$  of the filtered concentration field at this high  $Sc$ . Despite that for this  $Sc$ -number no data on the  $rms$  of the concentration are available, the results of our computation seem reasonable. Additionally the developed method is simple and straightforward and thus easy to integrate in existing codes.

For the future it is necessary to validate the model against DNS data of higher  $Sc$  number flows, especially the expected asymptotic behaviour of the cross stress term. Special care has also to be dedicated to the interaction between the numerics and the ADM model.

## REFERENCES

Batchelor, G. K., 1959. "Small-scale variation of convected quantities like temperature in turbulent fluid". Part 1. general discussion and the case of small conductivity. *J. Fluid Mech.* 5, 113–133.

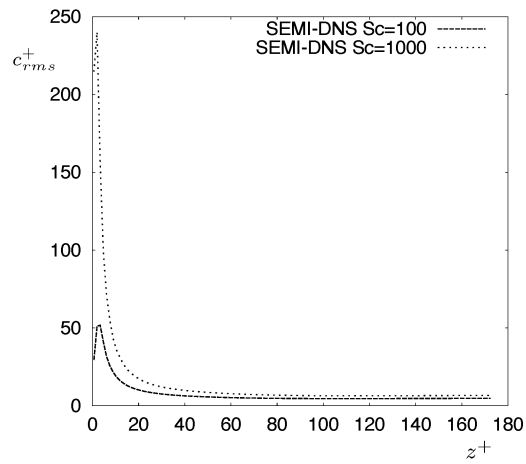


Figure 12:  $rms$  of the concentration at  $Sc = 100$  and  $Sc = 1000$

Domaradzki, J. A., Adams, N. A., 2002. "Direct modelling of subgrid scales of turbulence in large eddy simulations". *Journal o. Trubulence* 24 (3).

Kasagi, N., Iida, O., March 15-19 1999. Proceedings of the 5th ASME/JSME Joint Thermal Engineering Conference.

Na, Y., Hanratty, T. J., 2000. "Limiting behaviour of turbulent scalar transport close to a wall", *Int. J. of Heat and Mass Transfer* 43, 1749–1758.

Kim, J., Moin, P., Moser, R., 1987. "Turbulence statistics in fully developed channel flow at low Reynolds number". *J. Fluid Mech.* 177, 133–166.

Kobayashi, M. H., 1999. "On a class of Pade Finite Volume Methods", *J. of Comp. Physics.* 156, 137-180

Lele, S. K., 1992. "Compact finite difference schemes with spectral-like resolution". *J. Comp. Phys.* 103, 16–42.

Leonard, A., 1974. "Energy cascade in large eddy simulation of turbulent fluid flow". *Adv. Geophys.* 18A, 237-248

Manhart, M., 2004. "A zonal grid algorithm for DNS of turbulent boundary layers". *Computers and Fluids* 33 (3), 435–461.

Manhart, M., Friedrich, R., 2002. "DNS of a turbulent boundary layer with separation". *Int. J. Heat and Fluid Flow* 23 (5), 572–581.

Mathew, J., Lechner, R., Foysi, H., Friedrich, R., 2003. "An explicit filtering method for LES of compressible flows". *Phys. Fluids* 15 (8).

Na, Y., Hanratty, T. J., 2000. "Limiting behaviour of turbulent scalar transport close to a wall". *Int. J. of Heat and Mass Transfer* 43, 1749–1758

Na, Y., Papavassiliou, D. V., Hanratty, T. J., 1999. "Use of direct numerical simulation to study the effect of prandtl number on temperature field". *Int. J. Heat and Fluid Flow* 20, 187–195.

Shaw, D. A., Hanratty, T. J., 1977. "Turbulent mass transfer to a wall for large schmidt numbers". *A.I.Ch.E.J.* 23 (1), 28–37.

Stolz, S., Adams, N., 1999. "An approximate deconvolution procedure for large-eddy simulation". *American Institute of Physics*, 1699–1701.

Stolz, S., Adams, N. A., Kleiser, L., 2001. "An approximate deconvolution model for large-eddy simulation with application to incompressible wall-bounded flows". *Phys. Fluids* 13 (4), 997–1015.